

UC Santa Barbara

UC Santa Barbara Previously Published Works

Title

ZrO₂ gate dielectrics produced by ultraviolet ozone oxidation for GaN and AlGa_N/GaN transistors

Permalink

<https://escholarship.org/uc/item/0j0741pf>

Journal

Journal of Vacuum Science & Technology B, 24(2)

ISSN

1071-1023

Authors

Dora, Y
Han, S
Klenov, D
[et al.](#)

Publication Date

2006-03-01

Peer reviewed

ZrO₂ gate dielectrics produced by ultraviolet ozone oxidation for GaN and AlGaIn/GaN transistors

Yuvaraj Dora

Electrical and Computer Engineering Department, University of California, Santa Barbara, California 93106

Sooyeon Han

Materials Department, University of California, Santa Barbara, California 93106 and Department of Materials Science and Engineering, Korea Advanced Institute of Science and Technology, Gusung-dong, Yuseong-gu, Daejeon 305-701, Korea

Dmitri Klenov and Peter J. Hansen

Materials Department, University of California, Santa Barbara, California 93106

Kwang-soo No

Department of Materials Science and Engineering, Korea Advanced Institute of Science and Technology, Gusung-dong, Yuseong-gu, Daejeon 305-701, Korea

Umesh K. Mishra

Electrical and Computer Engineering Department, University of California, Santa Barbara, California 93106

Susanne Stemmer and James S. Speck^{a)}

Materials Department, University of California, Santa Barbara, California 93106

(Received 18 August 2005; accepted 29 December 2005; published 8 February 2006)

We investigated the suitability of ZrO₂ as a high-*k* dielectric for GaN material systems. Thin Zr films (4 nm) were deposited by electron-beam evaporation at room temperature on *n*-type GaN and Al_{0.22}Ga_{0.78}N (29 nm)/GaN high electron mobility transistor (HEMT) structures. The Zr-coated samples were subsequently oxidized at temperatures in the range of 200–400 °C in an ozone environment. Atomic force microscopy studies after oxidation show that the ZrO₂ forms a conformal layer on the underlying GaN template. Cross-section transmission electron microscopy studies showed little intermixing of the ZrO₂ with the AlGaIn/GaN. The relative dielectric constant of the ZrO₂ was determined to be 23. In comparison with HEMTs with bare gates (no dielectric between the gate metal and AlGaIn), the HEMTs with ZrO₂ showed two to three order of magnitude reduction in gate leakage current. Optimization of the HEMT process on sapphire substrates with ZrO₂ under the gates yielded devices with powers of 3.8 W/mm and 58% power-added efficiency at 4 GHz. © 2006 American Vacuum Society. [DOI: 10.1116/1.2167991]

I. INTRODUCTION

GaN has emerged as a promising material for the high-speed, high-power device applications. The large band gap and the high electron velocity make it suitable for high-power microwave applications.^{1,2} However, GaN metal-semiconductor field-effect transistor (MESFET) and AlGaIn/GaN high electron mobility transistor (HEMT) devices suffer from high gate leakage current which reduces the reliability and efficiency of the devices. High gate leakage current prevents the GaN MESFETs from reaching their potential for high-power levels.³ Field-effect transistors require low gate leakage current for low noise and improved reliability. Considerable interest in this issue has initiated the exploration of dielectrics to reduce the gate leakage in the GaN materials system.

GaN transistors suffer from a phenomenon called dc-to-rf dispersion, in which there is large signal current collapse at

high frequencies. This is related to the charging up of the surface states next to the drain side of the gate edge under high electric field. The surface states do not respond fast enough thereby affecting the high-frequency performance. One solution is to passivate the surface with plasma-enhanced chemical-vapor deposition (PECVD)-deposited SiN_x thus enabling high-power and high-frequency performance of GaN transistors.⁴ The gate dielectrics explored for GaN transistors should incorporate surface passivation to maintain the high-power and high-frequency performance.

It has been reported that the leakage occurs in GaN material through dislocations.^{5,6} Chini *et al.* have used a thin film of SiN_x grown *in situ* by metal-organic chemical-vapor deposition (MOCVD) to reduce gate leakage in GaN MESFETs.³ A 4 nm SiN_x was deposited on the sample surface by flowing disilane and ammonia inside the MOCVD chamber at a temperature of 980 °C. Chini *et al.* attributed the reduction in gate leakage with the SiN_x film due to reduced conduction through the dislocations or due to increased Schottky barrier height. SiO₂ deposited by PECVD

^{a)}Electronic mail: speck@mrl.ucsb.edu

under the gate has been shown to reduce gate leakage by six orders of magnitude in an AlGaIn/GaN HEMT structure.⁷ However, the low dielectric constant of SiO₂ ($\epsilon_r=3.9$) leads to a larger pinch-off voltage and reduced gate control in the HEMT.

In two separate studies Hansen *et al.* have reported the use of (Ba,Sr)TiO₃ (BST) (Ref. 8) and LiNbO₃ (Ref. 9) thin films deposited by rf-magnetron sputtering as possible dielectrics for GaN and AlGaIn/GaN devices. Hansen *et al.* performed a blanket deposition of the films just before the gate metallization step. However, they observed that the surface was damaged by the high ion energies associated with the sputtering process which resulted in reduced electron density and reduced electron mobility in the two-dimensional electron gas (2DEG) at the AlGaIn/GaN interface. Oxides such as crystalline gadolinium oxide (Gd₂O₃) and amorphous gadolinium gallium oxide Ga₂O₃(Gd₂O₃) have been tried in GaN devices using molecular-beam epitaxy to achieve low interface state density between the dielectric and the substrate.¹⁰ MgO and Sc₂O₃ deposited by rf plasma-assisted molecular-beam epitaxy have been tried as high-*k* gate dielectrics for AlGaIn/GaN devices.¹¹ The pulsed-IV curves reported in these studies show reduced dc-to-rf dispersion.^{11,12}

Thin metallic Zr and Hf films have been oxidized by ozone to yield high-*k* gate oxide dielectrics for Si and Si-Ge material systems.¹³ The ozone is generated by exposure of oxygen gas to ultraviolet (UV) radiation from a Hg vapor lamp. A high dielectric constant, large band gap ($E_g \sim 5.8$ eV), large conduction band offset with Si ($\Delta E_c \sim 1.4$ eV), and reduced charge trapping make these oxides a very promising dielectrics for Si.¹⁴ ZrO₂ is also reported to have breakdown fields above 3 MV/cm (Ref. 15) making it a potential candidate as a dielectric for large band gap, high-power material system such as GaN. The low-energy deposition of Zr followed by the UV-ozone oxidation at relatively lower temperatures could enable this film to be easily incorporated into the GaN process flow. In this article we report the use of ZrO₂ as a high-*k* dielectric for the GaN material system. Just before the gate metallization step, Zr was electron beam evaporated, followed by UV-ozone oxidation at 200–400 °C to produce a high-*k* gate dielectric. This method avoids energetic deposition of the oxide and high-temperature processing. Scanning transmission electron microscopy (STEM) showed that the oxide/III-nitride interface was abrupt. *CV* and *IV* measurements were performed to characterize the dielectric. The dc-to-rf dispersion was reduced by improved device fabrication. Power measurements were performed to study the compatibility of the oxide with the passivation and also to study the reliability of the dielectric in device performance.

II. EXPERIMENT

The deposition process for the ZrO₂ film was optimized by the analysis of metal-oxide semiconductor capacitor (MOSCAP) structure made on GaN and with surface characterization techniques. The optimized film was applied to

AlGaIn/GaN HEMTs, and the compatibility and performance of the film as a gate dielectric were tested in an actual device operation.

Si-doped *n*-type GaN templates on sapphire from LUMILOG were used as the substrates for the MOSCAP structure. The GaN layers were 3.5 μm thick with a carrier concentration in the range of 1×10^{18} – 3×10^{18} cm⁻³. The MOSCAP fabrication started with a lift-off metallization of Ti/Al/Ni/Au-20/120/30/50 nm and annealing at 870 °C in an N₂ environment in a rapid thermal annealer (RTA) to form Ohmic contacts to the *n*-GaN. The metal-oxide semiconductor (MOS) capacitors had a closed geometry, where the Ohmic contacts formed a ring around the Schottky contact. The surface was cleaned with O₂ plasma descum process for 30 s followed by an HCl dip for 40 s. The sample was immediately loaded into the electron-beam evaporator and pumped overnight to pressures as low as 8×10^{-7} torr. Thin films of Zr metal of various thicknesses (2–6 nm) were deposited. The samples were quickly transferred to the UV-ozone oxidation chamber with Hg lamps and a heated stage. The Hg vapor lamp emits wavelengths of 185 and 254 nm which are close to the bond energy of O₂. This radiation interacts with oxygen gas to produce oxygen radicals and ozone. This activated oxygen enhances the kinetics of oxidation compared to natural oxidation, resulting in better oxidation even at room temperature.¹⁶ Different oxidation temperatures (200–500 °C) and different oxidation times (15–60 min) were studied. After the oxidation, Pt/Au(100/200 nm) Schottky contacts were made by lift-off metallization. A schematic diagram of the MOSCAP process flow is shown in Fig. 1(a).

The optimized conditions for ZrO₂ on the MOS structures were used for the AlGaIn/GaN structures. The HEMTs had the following layer structure: Al_{0.22}Ga_{0.78}N(29 nm)/unintentionally doped GaN(UID GaN, 1.8 μm)/GaN:Fe (0.5 μm)/AlN(50 nm)/sapphire substrate. Room-temperature Hall measurements on the HEMT samples showed a 2DEG carrier concentration of 8×10^{12} cm⁻² and a mobility of ~ 1700 cm² V⁻¹ s⁻¹.

The HEMT fabrication started with the lift-off of the Ti/Al/Ni/Au (20/120/30/50 nm) Ohmic contact metallization and annealing at 870 °C in an N₂ environment for 30 s in the RTA. Mesa isolation of the devices was performed by removing about 120 nm of the structure by Cl₂-based reactive ion (RIE) etching. The sample surface was then cleaned by an O₂ plasma descum followed by a dip in HCl:DI = 1:2 for 30 s and a DI rinse to remove any native gallium oxide. The samples were pumped overnight in the electron-beam evaporator to a pressure of 9×10^{-7} torr. A 4 nm Zr film was electron beam deposited. The samples were then oxidized by the UV-ozone oxidation method as described earlier for 30 min at 300 °C. Ni/Au/Ni gates were defined by lift-off. In the AlGaIn/GaN HEMT samples, after the gate metallization the surface was passivated with PECVD-grown SiN_x of thickness 120 nm to remove dispersion. A schematic of the HEMT process flow is shown in Fig. 1(b).

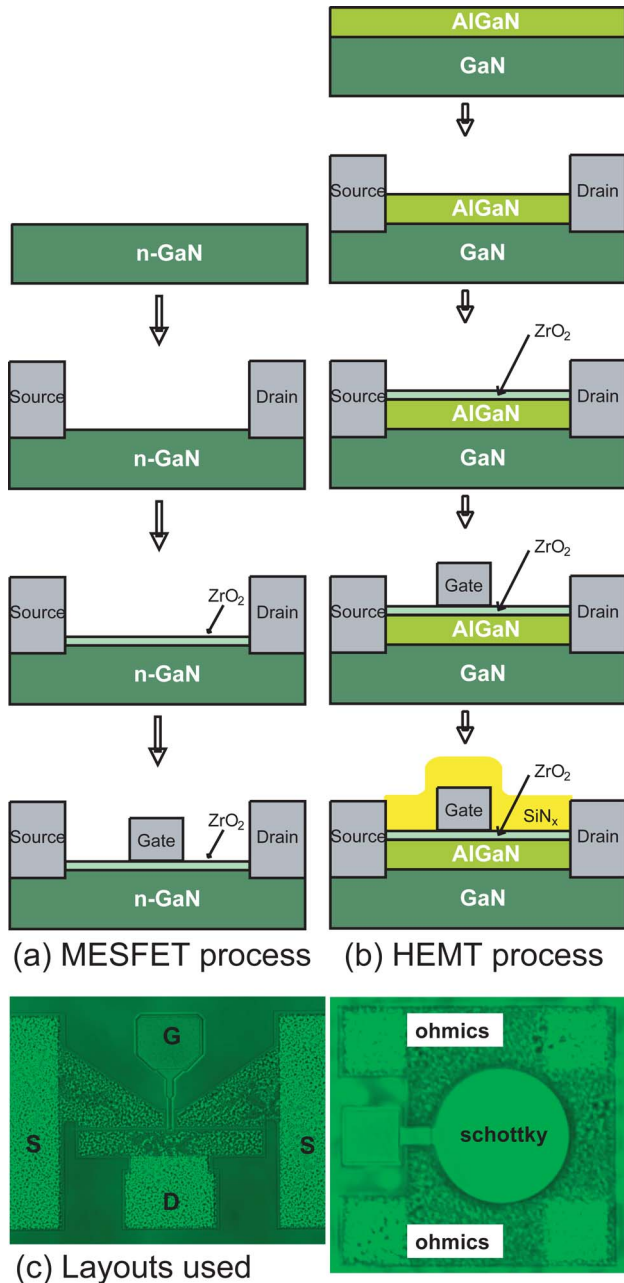


FIG. 1. MOSCAP and HEMT process flows. (a) MOSCAP process flow: *n*-GaIn substrate; Ohmic metallization and 870 °C alloying; Zr deposition and UV-ozone oxidation; gate metallization; (b) HEMT process flow: AlGaIn/GaIn HEMT structure; Ohmic metallization and 870 °C alloying; Zr deposition and UV-ozone oxidation; gate metallization; PECVD SiN_x passivation.

Structural characterization of the film was carried out with atomic force microscopy (AFM) and transmission electron microscopy (TEM). High-resolution TEM and high-angle annular dark-field scanning TEM (HRTEM and HAADF, respectively) images were obtained using a Tecnai F30-UT (FEI) field-emission TEM with $C_s=0.52$ mm operated at 300 kV. Cross-sectional TEM samples were prepared by conventional techniques including ion milling at 3.5 kV and liquid-nitrogen temperature using a Fischione ion mill. Capacitance-voltage measurements were performed with

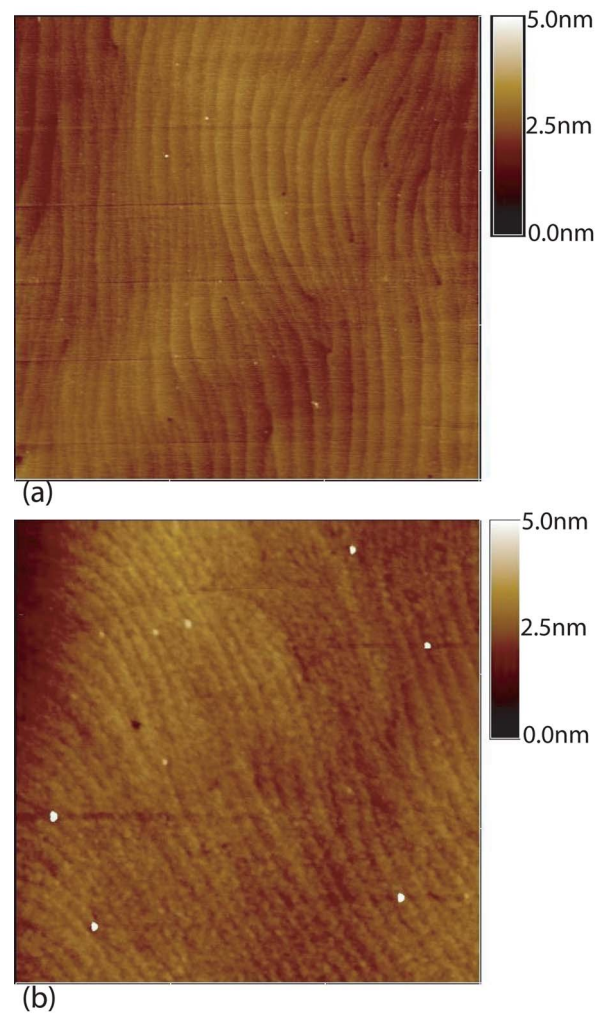


FIG. 2. (a) AFM scan of the MOSCAP sample surface just before Zr deposition; (b) AFM scan of the MOSCAP sample surface after Zr deposition and UV-ozone oxidation. $3 \times 3 \mu\text{m}^2$ scan size.

Keithley-590 CV meter at 1 MHz. There was no significant shift between the forward and reverse sweeps which showed that there was no significant charge trapping in the oxide film or at the oxide/III-nitride interface. The leakage current measurements were made using HP 4145 semiconductor parameter analyzer.

The test structures on the HEMT samples consisted of the HEMT devices and circular CV pattern with a guard ring [Fig. 1(c)]. The gate width and gate length of the transistors measured were 150 and 0.7 μm , respectively. The source-to-drain spacing was 3.4 μm . Electrical characterization included CV, gate leakage, and pulsed-IV and load-pull power measurements. The load-pull power measurements on the HEMTs were performed on a Maury 2–18 GHz load-pull system.

III. RESULTS AND DISCUSSION

For the MOSCAP structure, we examined the surface of the GaIn at various process steps. Figure 2(a) shows the GaIn surface after the Ohmic anneal and the mesa isolation etch,

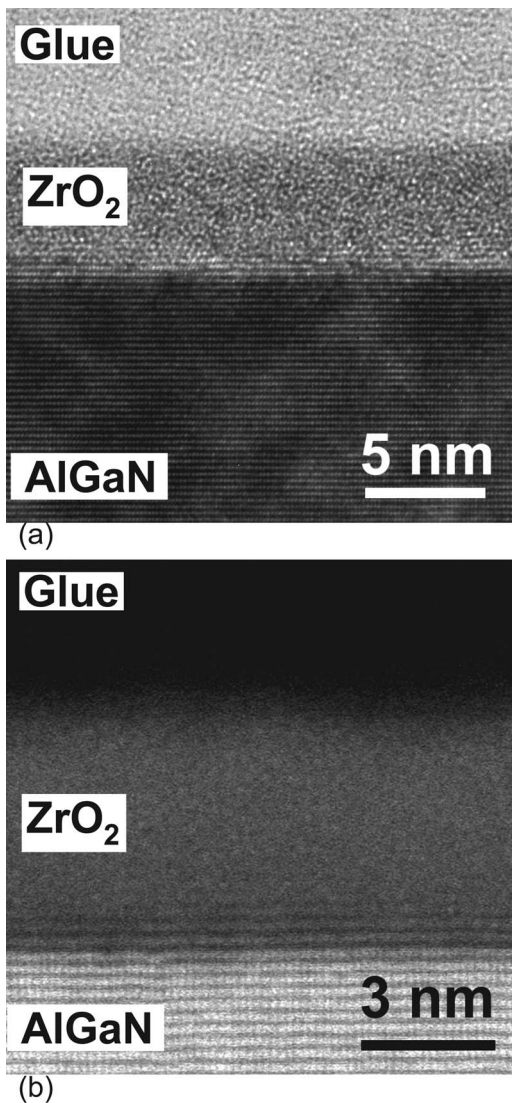


FIG. 3. (a) HRTEM image showing an abrupt interface between ZrO₂ and AlGaIn without any reaction layer; (b) HAADF-STEM image showing a greater roughness of the AlGaIn surface, possibly due to a degree of oxidation during the ozone oxidation.

but just prior to the Zr deposition. The GaN surface showed a well-defined step-terrace structure. After Zr deposition and UV oxidation at 200 °C, the ZrO₂-coated GaN surface still showed some evidence of the steps [Fig. 2(b)]. Thus, the UV-ozone process appeared to produce a thin uniform conformal oxide.

Cross-sectional TEM micrographs confirmed a uniform thickness of the ZrO₂ film of approximately 5 nm. Both HRTEM and HAADF-STEM images showed that the ZrO₂ was amorphous. In addition, no crystallization was observed by nanodiffraction. However, some degree of nanocrystallinity could not be excluded.¹⁷ HRTEM images [Fig. 3(a)] showed an abrupt interface between AlGaIn and ZrO₂ and no reaction layer was found. The HAADF-STEM images [Fig. 3(b)] showed the absence of any reaction layer between AlGaIn and ZrO₂ though a greater roughness of the AlGaIn surface was observed than expected, which may be due to some

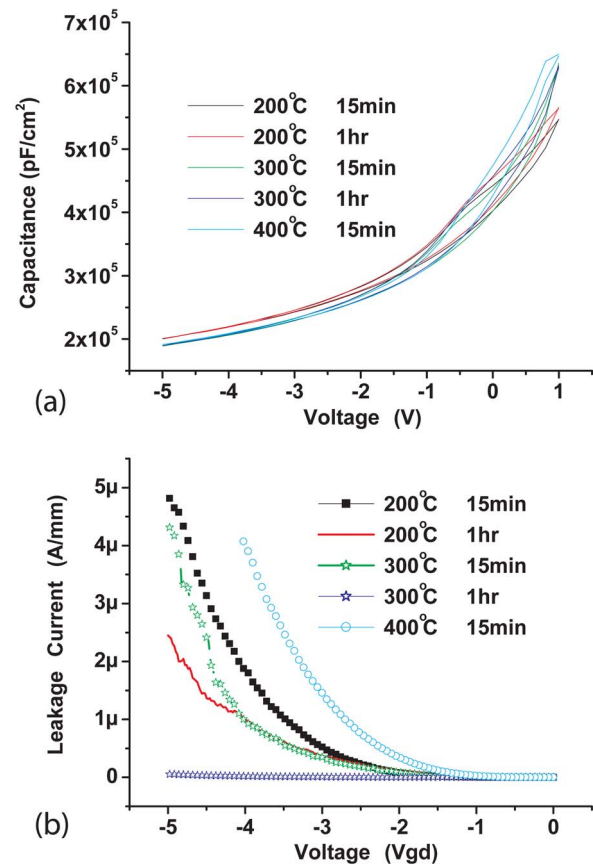


FIG. 4. (a) CV measurements and (b) leakage measurements for the MOS capacitor for ZrO₂ oxidation conditions: 200 °C, 15 min; 200 °C, 1 h; 300 °C, 15 min; 300 °C, 1 h; 400 °C, 15 min.

degree of oxidation of the AlGaIn during ozone oxidation. Direct evidence of the oxidation of AlGaIn is not available. X-ray photoemission spectroscopy (XPS) done on MESFET sample did not show peak shifts of the Ga 2*p* typical for the oxidation.

Figure 4(a) shows the CV characteristics of a 2.5 nm film of Zr under the UV oxidation conditions of different temperature and time. The maximum capacitance was in the range of 6×10^5 pF cm⁻². Comparing the capacitance and the trapping characteristics [Fig. 4(a)] indicated that higher temperature and longer time for UV oxidation resulted in a very small increase in the capacitance. Figure 4(b) shows the IV curve of these MOSCAP devices. Among several UV conditions, the post-deposition annealed device after UV oxidation at 300 °C for 1 h showed the best result based on the lowest reverse bias currents.

In AlGaIn/GaN HEMTs, PECVD deposition of the SiN_x passivation layer on the surface of the AlGaIn is performed at 250 °C. Therefore to sustain a high-quality SiN_x passivation, it is necessary that the temperature and the time for which the passivation layer and the AlGaIn surface is subjected to oxidation should be limited to as close to 250 °C as possible. So an optimum temperature of 300 °C and a time of 30 min

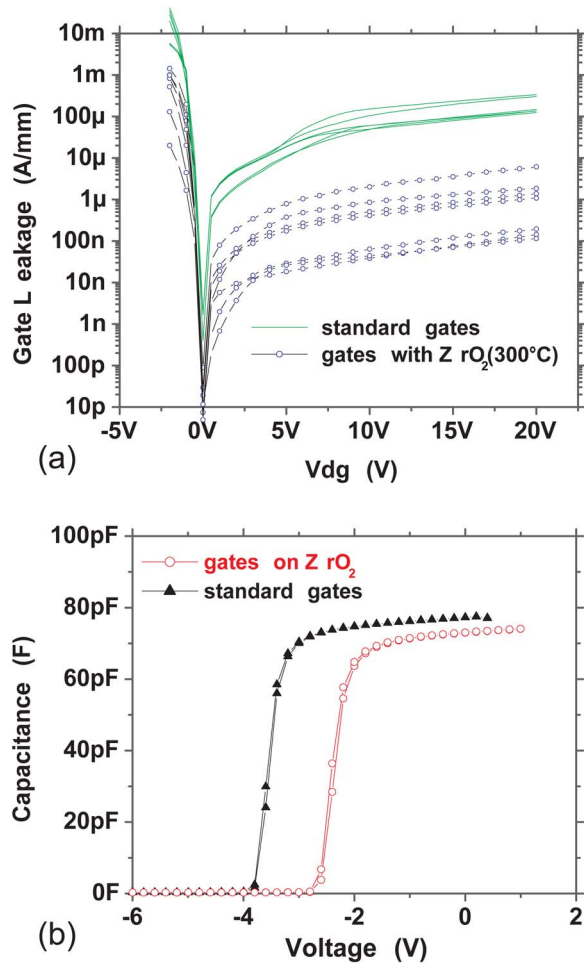


FIG. 5. (a) Comparison of gate leakage in HEMTs without ZrO₂ (standard gates) and with ZrO₂. (b) CV measurement of capacitors made on HEMT structure which show very little shift in the gate-2DEG capacitance confirming a dielectric with high k . The small hysteresis between forward and reverse biases is indicative of insignificant charge trapping by the dielectric. The shift in threshold voltage is due to the reduction in the polarization-induced 2DEG charge density. The area of the capacitor was $2.55 \times 10^4 \mu\text{m}^2$.

for the UV oxidation step were chosen for all the AlGa_{0.2}N/GaN HEMT samples so that the passivation would not be seriously affected.

The gate leakage in the AlGa_{0.2}N/GaN HEMTs was reduced by at least two orders of magnitude with ZrO₂ under the gates [Fig. 5(a)]. All gate leakage measurements were performed after the devices were passivated with SiN_x. After passivation, the dc-to-rf dispersion was reduced, but the peak electric field increased because all the electric-field lines terminate at the drain edge of the gate. Thus, measurements of gate leakage after passivation ensured that the high electric field at the drain side of the gate was the same as in the high-frequency, high-power operation of HEMTs. Figure 5(b) compares the CV measurements with and without ZrO₂ under the gate. By comparing the capacitance values at a gate bias for which there is still an undepleted 2DEG, the relative dielectric constant for the ZrO₂ layer was extracted to be $\epsilon_{\text{ZrO}_2} = 23$. This value of dielectric constant agreed with

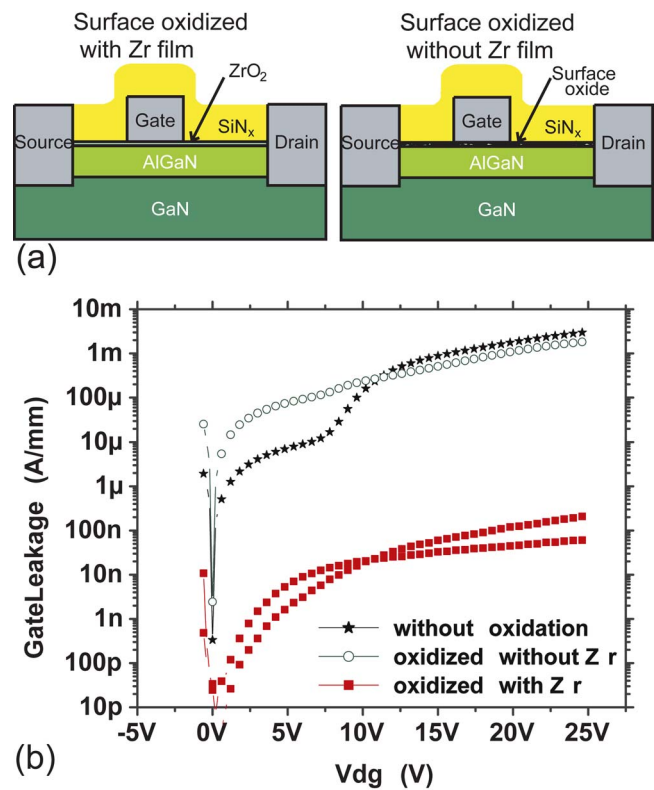


FIG. 6. (a) Schematic showing the devices used in a controlled experiment to check whether the leakage reduction is due to ZrO₂ or due to oxidized AlGa_{0.2}N. (b) Leakage measurements from the controlled experiment which show that the leakage reduction is due to ZrO₂ and not due to the oxidation of AlGa_{0.2}N.

the numbers reported by others for amorphous ZrO₂.^{14,18} The absence of any significant shift in the CV curve between the positive and negative sweeps demonstrated that the ZrO₂-AlGa_{0.2}N interface had insignificant charge trapping. The global shift in the CV curve towards the right, exhibiting a reduced pinch-off voltage, is attributed to the reduction in the 2DEG concentration at zero gate bias after the oxidation process, suggesting a change in surface Fermi-level position at the AlGa_{0.2}N/ZrO₂ interface. However, the reduction in the zero-bias 2DEG concentration did not affect the device performance, because with ZrO₂ the device could be biased to more positive voltages, thus inducing additional 2DEG concentration.

To verify whether the gate leakage reduction was due to ZrO₂ or due to surface oxidation of AlGa_{0.2}N, a controlled experiment was performed. One of the samples was partially shadow masked during the electron-beam evaporation of Zr. Thus part of the sample had Zr deposited on it and the rest had the bare AlGa_{0.2}N surface. The entire sample was oxidized by the UV-ozone oxidation method at 300 °C for 30 min. Gates were deposited in both the regions, and the SiN_x passivation was performed to reduce dispersion. Figure 6 shows the gate leakage comparison of the AlGa_{0.2}N surface, oxidized with and without Zr. This controlled experiment clearly showed that the leakage reduction was due to ZrO₂ and not due to surface oxidation of AlGa_{0.2}N.

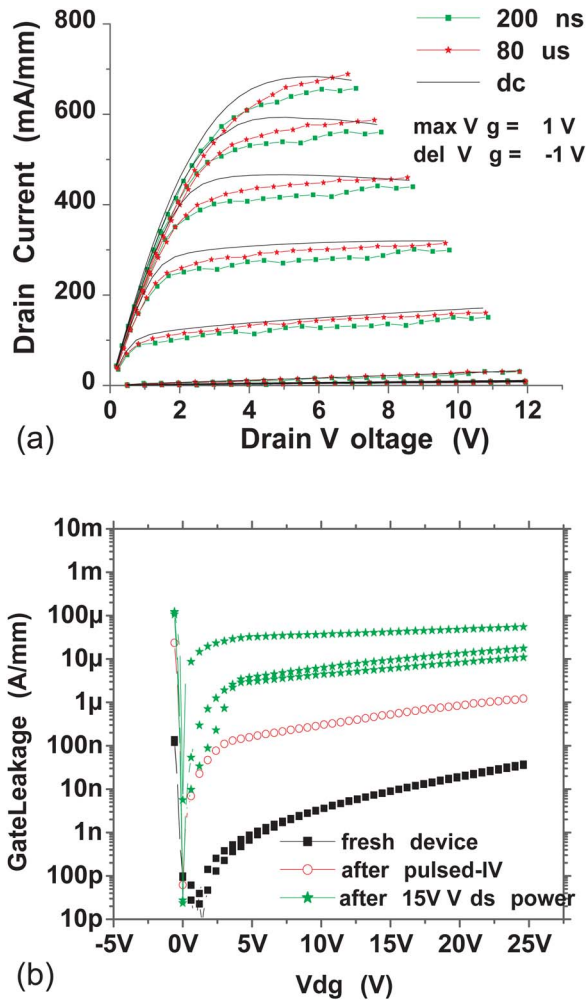


FIG. 7. (a) Pulsed-IV measurements show that the high-frequency current is reduced compared to the dc current, a phenomenon referred to as “dispersion” in AlGaIn/GaN HEMTs. (b) Degradation observed in gate leakage with pulsed-IV measurements and 4-GHz load-pull power measurements.

Two challenges for using ZrO₂ as gate dielectric for AlGaIn/GaN HEMTs were observed. One was the effectiveness of the SiN_x passivation in the AlGaIn/GaN HEMTs in the presence of a gate dielectric. Figure 7(a) shows the high-frequency pulsed-IV curves showing knee walkout compared to the dc IV curves, commonly referred to as dispersion. Due to the poor thermal conductivity of the sapphire substrate, a well-passivated AlGaIn/GaN HEMT grown on sapphire substrate is expected to have a peak pulsed current at least 10% above that of the peak dc current. The pulsed-IV curves show lower current level than the dc current level indicating the presence of dispersion. Another issue is the stability of the gate dielectric in device operation. Figure 7(b) shows that the gate leakage is degraded after pulsed-IV measurements and 4 GHz load-pull power measurements at a bias of V_{ds} = 15 V.

To address the issues of dispersion and the dielectric stability, the fabrication process of the AlGaIn/GaN HEMT was changed as shown in Fig. 8(a). Instead of passivating the HEMT after the gate metal deposition, SiN_x was deposited

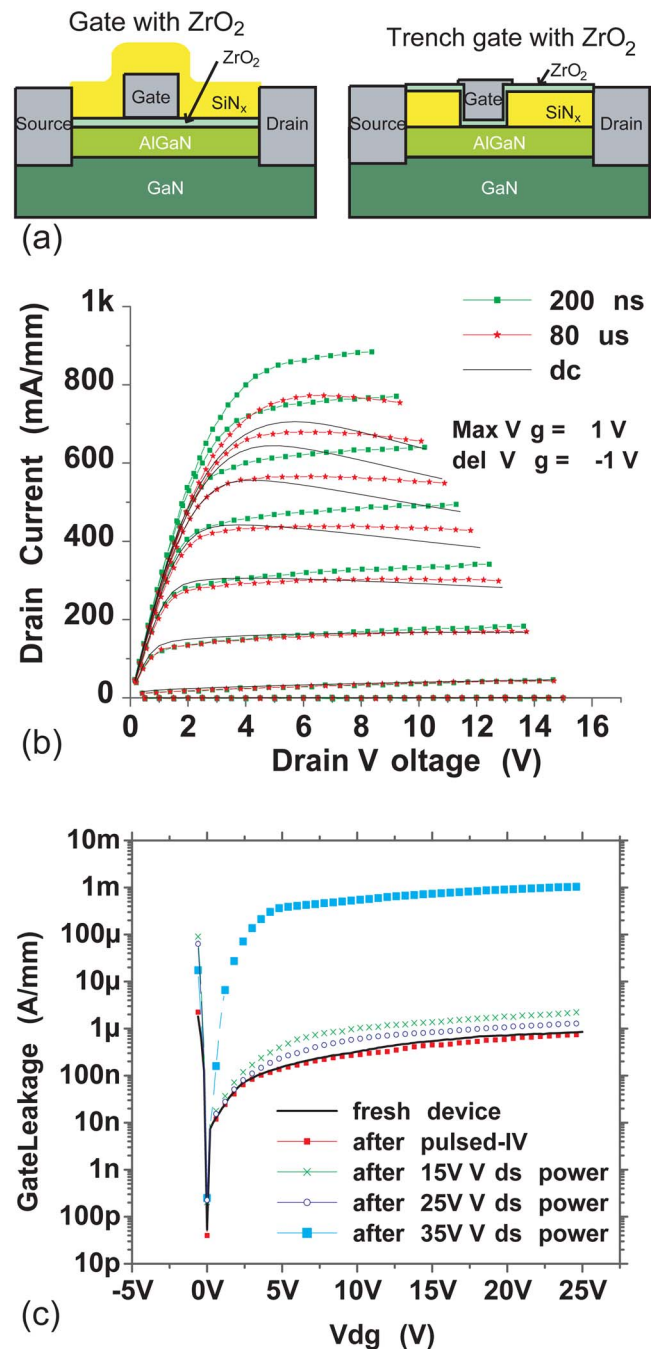


FIG. 8. (a) Schematic showing the improved fabrication, where the SiN_x passivation layer was deposited first, and then the ZrO₂ was formed in the trench etched in the passivation layer. (b) Pulsed-IV measurements show that the high-frequency current is higher than the dc current, attributed to the removal of dispersion and to the poor heat-sinking capacity of the sapphire substrate. (c) Gate leakage did not degrade in the 4-GHz power measurements until a V_{ds} bias of 35 V was applied.

first. Using the gate lithography, trenches were etched in the SiN_x, and the photoresist was removed. After solvent cleaning, Zr was blanket deposited and oxidized as described earlier. Finally with another gate lithography aligned towards the drain side wall of the trench, the gate metal was deposited, introducing a field-plate effect.^{1,19}

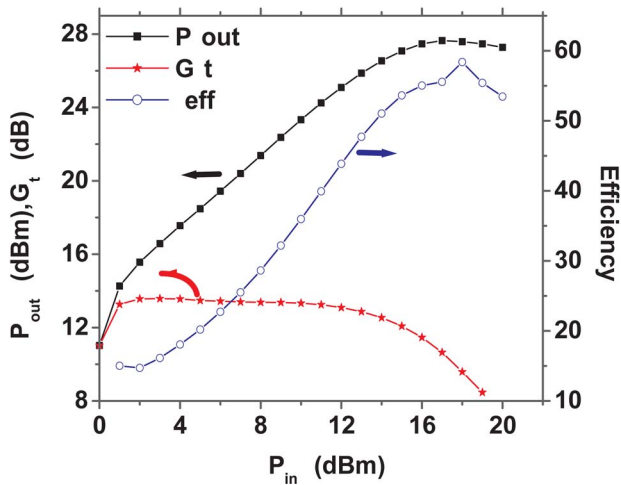


FIG. 9. Power measurements at 4 GHz on the HEMT with ZrO₂ on sapphire substrate gave a maximum power of 3.8 W/mm for a bias of $V_{ds}=25$ V. The power-added efficiency was 58%.

The pulsed-IV curves shown in Fig. 8(b) demonstrate improved passivation. The 200 ns pulsed current was 20% higher than the dc current level showing very good passivation for a AlGaIn/GaN HEMT on a substrate which has a poor thermal conductivity. Power measurements at 4 GHz showed a peak power of 3.8 W/mm at a bias of $V_{ds}=25$ V for a HEMT on sapphire substrate (Fig. 9). The power-added efficiency (PAE) for this power was 58%. The high-power and PAE results at 4 GHz are another indication of insignificant high-frequency dispersion in the devices. Collectively, these results confirm the applicability of ZrO₂ as gate dielectric for high-frequency operation.

Figure 8(c) shows that the gate leakage reduction did not degrade until the power measurements at V_{ds} bias of 35 V. We believe that the improvement in the gate leakage degradation is caused by a reduced field peaking, due to the field-plate effect caused by the alignment of the gate edge over the wall of the SiN_x trench. After the device showed degradation in the gate leakage, the pulsed-IV and load-pull measurements were performed. After the degradation, however, the current levels and the power levels in the devices did not change. However, the gate leakage was significantly higher after the degradation, but was on the same order as a device without any dielectric under the gate. This leads us to believe that the dielectric degraded under very high field operation. Further investigation is necessary to improve further the high-field reliability of this dielectric.

IV. CONCLUSIONS

We have investigated the suitability of ZrO₂ as a high- k dielectric for GaN material system. We optimized the conditions of Zr deposition and the UV-ozone oxidation on GaN MOS structures. Structural characterization showed that there was little intermixing of the dielectric with GaN. The

optimized conditions were used to apply ZrO₂ as gate dielectric to AlGaIn/GaN HEMTs. The compatibility of ZrO₂ with the issue of dispersion removal in AlGaIn/GaN HEMTs by SiN_x passivation was studied with the help of pulsed-IV measurements and load-pull power measurements at 4 GHz. The reliability of the dielectric with the device operation was also studied. A better process technique yielded improved passivation, and hence higher microwave power. The improved process also resulted in improved reliability of the dielectric. These experiments show the potential and suitability of ZrO₂ as a high- k gate dielectric for AlGaIn/GaN structures.

ACKNOWLEDGMENTS

The authors gratefully acknowledge the support of DARPA, CNID, and SRC programs at UCSB. This work made use of the Materials Research Lab (MRL) Central Facilities supported by the MRSEC program of the National Science Foundation under Award No. DMR00-80034.

- ¹A. Chini, D. Buttari, R. Coffie, L. Shen, S. Heikman, A. Chakraborty, S. Keller, and U. K. Mishra, *IEEE Electron Device Lett.* **25**, 229 (2004).
- ²Y.-F. Wu, A. Saxler, M. Moore, R. P. Smith, S. Sheppard, P. M. Chavarkar, T. Wisleder, U. K. Mishra, and P. Parikh, *IEEE Electron Device Lett.* **25**, 117 (2004).
- ³A. Chini, J. Wittich, S. Heikman, S. Keller, S. P. DenBaars, and U. K. Mishra, *IEEE Electron Device Lett.* **25**, 55 (2004).
- ⁴U. K. Mishra, P. Parikh, and Y. Wu, *Proc. IEEE* **90**, 1022 (2002).
- ⁵P. Kozodoy, J. P. Ibbetson, H. Marchand, P. T. Fini, S. Keller, J. S. Speck, S. P. Denbaars, and U. K. Mishra, *Appl. Phys. Lett.* **73**, 975 (1998).
- ⁶E. J. Miller, X. Z. Dang, and E. T. Yu, *J. Appl. Phys.* **88**, 5951 (2000).
- ⁷M. A. Khan, X. Hu, A. Tarakji, G. Simin, J. Yang, R. Gaska, and M. S. Shur, *Appl. Phys. Lett.* **77**, 1339 (2000).
- ⁸P. J. Hansen, L. Shen, Y. Wu, A. Stonas, Y. Terao, S. Heikman, D. Buttari, T. R. Taylor, S. P. DenBaars, U. K. Mishra, R. A. York, and J. S. Speck, *J. Vac. Sci. Technol. B* **22**, 2479 (2004).
- ⁹P. J. Hansen, Y. Terao, Y. Wu, R. A. York, U. K. Mishra, and J. S. Speck, *J. Vac. Sci. Technol. B* **23**, 162 (2005).
- ¹⁰B. P. Gila, K. N. Lee, W. Johnson, F. Ren, C. R. Abernathy, S. J. Pearton, M. Hong, J. Kwo, J. P. Mannaerts, and K. A. Anselm, *Proceedings of the IEEE-Cornell Conference on High Performance Devices* (IEEE, New York, 2000), p. 182.
- ¹¹R. Mehandru, B. Luo, J. Kim, F. Ren, B. P. Gila, A. H. Onstine, C. R. Abernathy, S. J. Pearton, D. Gotthold, R. Birkhahn, B. Peres, R. Fitch, J. Gillespie, T. Jenkins, J. Sewell, D. Via, and A. Crespo, *Appl. Phys. Lett.* **82**, 2530 (2003).
- ¹²B. Luo, J. W. Johnson, J. Kim, R. M. Mehandru, F. Ren, B. P. Gila, A. H. Onstine, C. R. Abernathy, S. J. Pearton, A. G. Baca, R. D. Briggs, R. J. Shul, C. Monier, and J. Han, *Appl. Phys. Lett.* **80**, 1661 (2002).
- ¹³S. Ramanathan, P. C. McIntyre, S. Guha, and E. Gusev, *Appl. Phys. Lett.* **84**, 389 (2004).
- ¹⁴G. D. Wilk, R. M. Wallace, and J. M. Anthony, *J. Appl. Phys.* **89**, 5243 (2001).
- ¹⁵J. Shappir, A. Anis, and I. Pinsky, *IEEE Trans. Electron Devices* **33**, 442 (1986).
- ¹⁶S. Ramanathan, G. D. Wilk, D. A. Muller, C. M. Park, and P. C. McIntyre, *Appl. Phys. Lett.* **79**, 2621 (2001).
- ¹⁷M.-Y. Ho, H. Gong, G. D. Wilk, B. W. Busch, M. L. Green, P. M. Voyles, D. A. Muller, M. Bude, W. H. Lin, A. See, M. E. Loomans, S. K. Lahiri, and P. I. Ralsanen, *J. Appl. Phys.* **93**, 1477 (2003).
- ¹⁸S. Ramanathan, C. Park, and P. C. McIntyre, *J. Appl. Phys.* **91**, 4521 (2002).
- ¹⁹H. Xing, Y. Dora, A. Chini, S. Heikman, S. Keller, and U. K. Mishra, *IEEE Electron Device Lett.* **25**, 161 (2004).